JOURNAL OF MATERIALS SCIENCE **36** (2001) 2539–2545

Ac conductivity of $BaTiO_3$ containing $(90V_2O_5\text{-}10P_2O_5)$ oxide glasses dispersed with nanocrystalline particles

D. K. MODAK, U. K. MANDAL, M. SADHUKHAN, B. K. CHAUDHURI*
Solid State Physics Department, Indian Association for the Cultivation of Science, Calcutta 700032, India
E-mail: sspbkc@mahendra.iacs.in

T. KOMATSU
Department of Chemistry, Nagaoka University, Nagaoka, Japan

The frequency dependent AC conductivity (σ_{ac}) of some new multicomponent $(1-x)$ $(90V_2O_5\text{-}10P_2O_5) + xBaTiO_3$ ($x = 0.1$ to 0.9) type glasses containing nanocrystalline $BaTiO_3$ particles (observed from the transmission electron microscopic study) has been reported in the temperature range 80–400 K. The behavior of σ_{ac} is broadly similar to what has been observed previously in many other amorphous semiconductors and polymers (namely nearly linear frequency dependence and weak temperature dependence). Analysis of the experimental conductivity data shows that Long's overlapping large polaron tunneling (OLPT) mechanism is the most probable mechanism of conduction for the present $BaTiO_3$ doped glasses. The Quantum mechanical tunneling (QMT) model and the classical hopping of electrons over a barrier can, however, explain the AC conductivity data only below $\theta_D/2$–160 K (θ_D is the Debye temperature). Reasonable values of the relaxation time and barrier heights related to the models have been obtained from the fits of the conductivity data. © *2001 Kluwer Academic Publishers*

1. Introduction

Transition metal oxide (TMO) glasses are interesting because of their probable applications in threshold and memory switching as well as in other applications like cathode materials [1–3]. These glasses show more than one valence state for the transition metal ions [4]. Frequency dependent AC conductivity and loss have been reported in many semiconducting glasses with transition metal ions [5–7]. However, the experimental results of frequency dependent conductivity are not beyond controversy. At low temperature, the AC conductivity $\sigma_{ac}(\omega)$ at frequency ω behaved as ω^s where s is generally less than unity and depends on temperature. A value of s, power low exponent, larger than unity has also been reported [8–10] even at low frequencies and temperature. Many models [4, 11, 12] based on relaxation caused by the hopping or tunneling of electrons or atoms between equilibrium sites have been developed to explain the frequency and temperature dependent AC conductivity and the frequency power law exponent s. However, these models are applicable only within a limited temperature range. Apart from the controversy of the low temperature behavior of $\sigma(\omega)$ and s, there is some uncertainty [13] whether a Debye-type dielectric loss peak exists at higher temperatures, where the conductivity approaches the DC conductivity [$\sigma(\omega = 0)$].

There are several publications on the electrical properties of the vanadate glasses with conventional network formers like P_2O_5, SiO_2 [5, 14–16], but very little work has been done on the vanadate glasses with ferroelectric $BaTiO_3$, $SrTiO_3$ etc. oxides. Recently such glasses have been prepared in our laboratory and found to show very large dielectric permittivity [17]. This is because of the presence of nano/microcrystalline $BaTiO_3$, $SrTiO_3$, TiO_2 etc. phases embedded in the base glass matrix. Partial annealing of these glasses (around 500 K for three hours) increases the nanostructure and shows relaxor-type ferroelectric transition around 390 K [18]. These glasses are, therefore, a special type of glass-ceramic nanocomposites. Study of AC conductivity and other properties of this new type of glassy material appears to be interesting

The purpose of the present paper is to study the frequency dependent AC conductivity in the $(1-x)(90V_2O_5\text{-}10P_2O_5) - xBaTiO_3$ glasses containing nanocrystalline $BaTiO_5$ phase and also to study the influence of the $BaTiO_3$ on the frequency dependent electrical properties of these unconventional glasses over a wide range of frequency (500–10^4 Hz) and temperature (80–400 K). X-Ray diffraction, DTA, infra-red and transmission electron microscopic studies have also been made to characterize these glasses. The AC relaxation

* Author to whom all correspondence should be addressed.

mechanism in these glasses and some annealed glasses will be reported elsewhere.

2. Experimental

The ferroelectric $BaTiO_3$ doped vanadium phosphate glasses viz. $(1-x)(90V_2O_5\text{-}10P_2O_5) + x\,BaTiO_3$ with $x = 0.1$, 0.3, 0.5, 9.0 and 0.9 mol % of $BaTiO_3$ (hereafter these glasses are denoted by VPBT) have been prepared by melt-quenching technique [19]. The raw materials V_2O_5, $NH_4H_2PO_4$ and $BaTiO_3$ with high purity (99.99%) are mixed in appropriate proportions and melted in air under atmospheric condition in platinum crucibles at 950–1000°C, depending on $BaTiO_3$ concentrations, for one hour. The melt is then quenched at room temperature between two copper blocks. The amorphous character of all these samples was examined by X-ray diffraction (XRD) and scanning electron microscopic studies. To find the presence of nanocrystals embedded in the glass matrix transmission electron microscopic studies of the glass powders on carbon-coated grids were made. The glass transition temperatures (T_g) are estimated by differential thermal analysis with heating rate of 10°C/min. The infra-red absorption spectra of the glasses with KBr have also been studied to characterize the glasses.

The densities of the sample were measured by using benzene as an immersion liquid. Room temperature (298 K) paramagnetic susceptibilities of the glasses were also measured by VSM. Some important parameters of the glasses are shown in Table I. The frequency dependent AC measurement was carried out with Gen Rad capacitance bridge in the frequency range (100–10^4 Hz). All measurements were made in the temperature range of 80–400 K using a cryostat and temperature controller with an accuracy of ±0.5 K similar to our earlier work [23]. For the AC conductivity $\sigma_{ac}(\omega)$ measurements, the glass samples each of diameter ∼8 mm and thickness ∼1 mm are used. After polishing the two faces, they are coated with gold using sputtering technique. The conductivity measurements for a particular sample at two different runs were found to vary by about ±2%. Room temperature thermoelectric power measurements of all the glasses indicated electrons as the carriers.

3. Results

The X-ray diffraction patterns (with Cu K_α radiation) of some of the as quenched $(1-x)\,(90V_2O_5\text{-}10P_2O_5) + x\,BaTiO_3$ glasses (with $x = 0.3$, 0.9 and 0.95) are shown in Fig. 1a to c indicating glassy character. The DTA curves of the samples, shown in Fig. 2a to d for different compositions of the glasses, are used to find the glass transition temperature (T_g) and the crystallization temperature (T_x) shown in Table I. The infrared spectra of all $BaTiO_3$ doped glasses (between 400–4000 cm^{-1})

TABLE I Some physical parameters of the $(1-x)(90V_2O_5\text{-}10P_2O_5) + x\,BaTiO_3$ glasses

Value of x	ρ (gm cm^{-3})	T_g (°C)	T_x (°C)
0.1	3.01	240	250
0.3	2.98	245	250
0.5	3.02	248	255
0.9	3.38	250	295

The estimated maximum errors in the measurements of density (ρ), T_g, and T_x are, respectively, ±2%, ±3% and +3%.

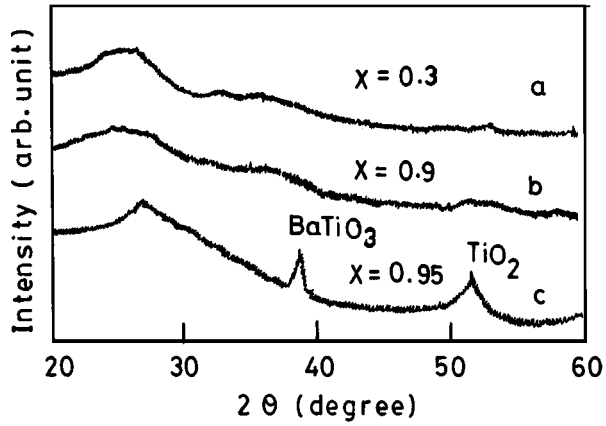

Figure 1 X-ray diffraction patterns (with Cu K_α radiation) of the as quenched $(1-x)(90V_2O_5\text{-}10P_2O_5) + x\,BaTiO_3$ glasses for (a) $x = 0.3$, (b) 0.9 and (c) 0.95.

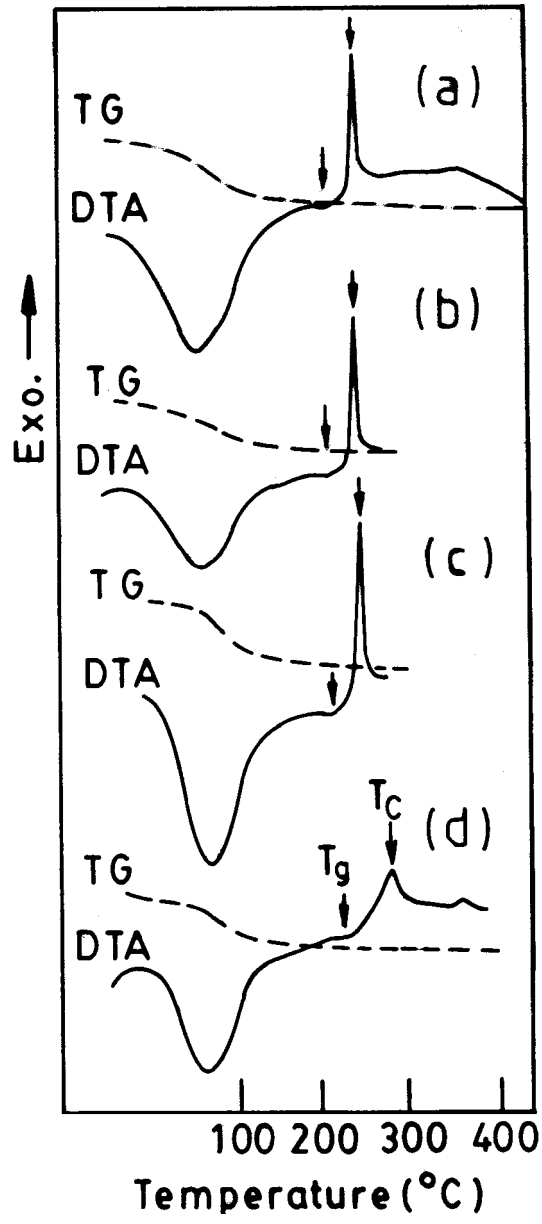

Figure 2 DTA curves of $(1-x)\,(90V_2O_5\text{-}10P_2O_5) + x\,BaTiO_3$ glasses for (a) $x = 0.1$, (b) $x = 0.3$, (c) $x = 0.5$ and (d) $x = 0.9$.

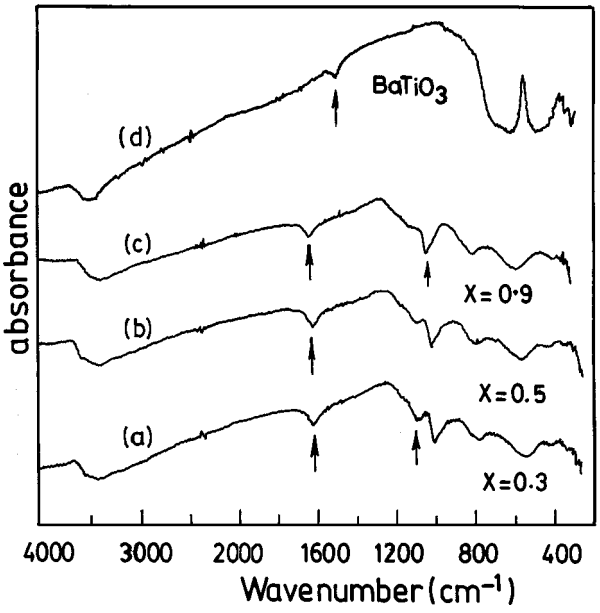

Figure 3 Infrared absorption spectra of some of the $(1-x)(90V_2O_5$-$10P_2O_5)+xBaTiO_3$ glasses and $BaTiO_3$: (a) $x=0.3$, (b) $x=0.5$, (c) $x=0.9$ and (d) pure $BaTiO_3$.

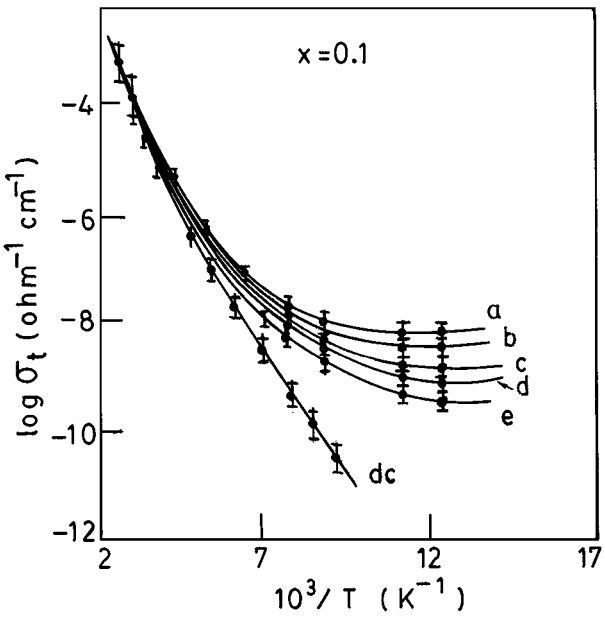

Figure 4 The thermal variation of logarithmic of total conductivity (σ_t) for the $(1-x)$ $(90V_2O_5$-$10P_2O_5)+xBaTiO_3$ glass with $x=0.1$ at 10.0 (a), 5.0 (b), 2.0 (c), 1.0 (d) and 0.5 kHz (e), respecrtively, along with the DC conductivity. Solid lines with error bars are guides for the eyes.

are shown in Fig. 3 for comparison. Fig. 4 shows the variation of angular frequency (ω) dependent total conductivity ($\sigma_t=\sigma_{ac}+\sigma_{dc}$) of a typical $BaTiO_3$ doped VPBT glass with $x=0.1$ as a function of inverse temperature measured at different frequencies. The temperature dependent DC conductivity (σ_{dc}) of this glass is also shown in the same Fig. 4 . The frequency (ω) dependent AC conductivity (obtained by subtracting DC conductivity from the total conductivity) is plotted in Fig. 5 for the same glass sample (with $x=0.1$) at various fixed values of low temperatures where DC conductivity is negligibly small. From the slopes of $\log\sigma_{ac}(\omega)$ vs. $\log\omega$ curves (Fig. 5), the values of the power law exponent s are estimated and plotted in Fig. 6 as a function

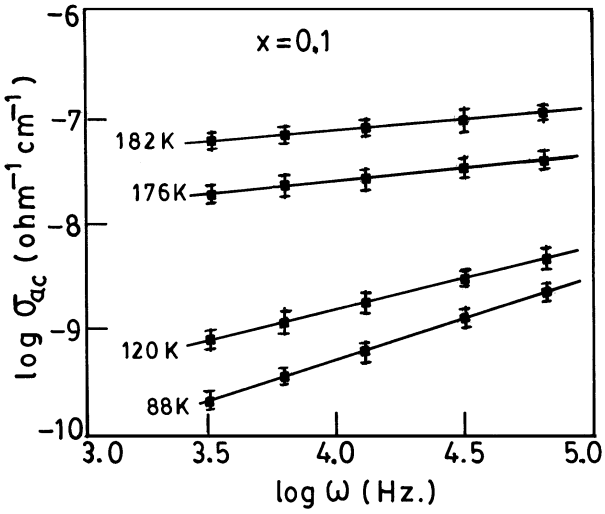

Figure 5 Frequency dependent AC conductivity of a VPBT glass sample with $x=0.1$ at different fixed temperatures. Continuous lines with error bars are guides for the eyes.

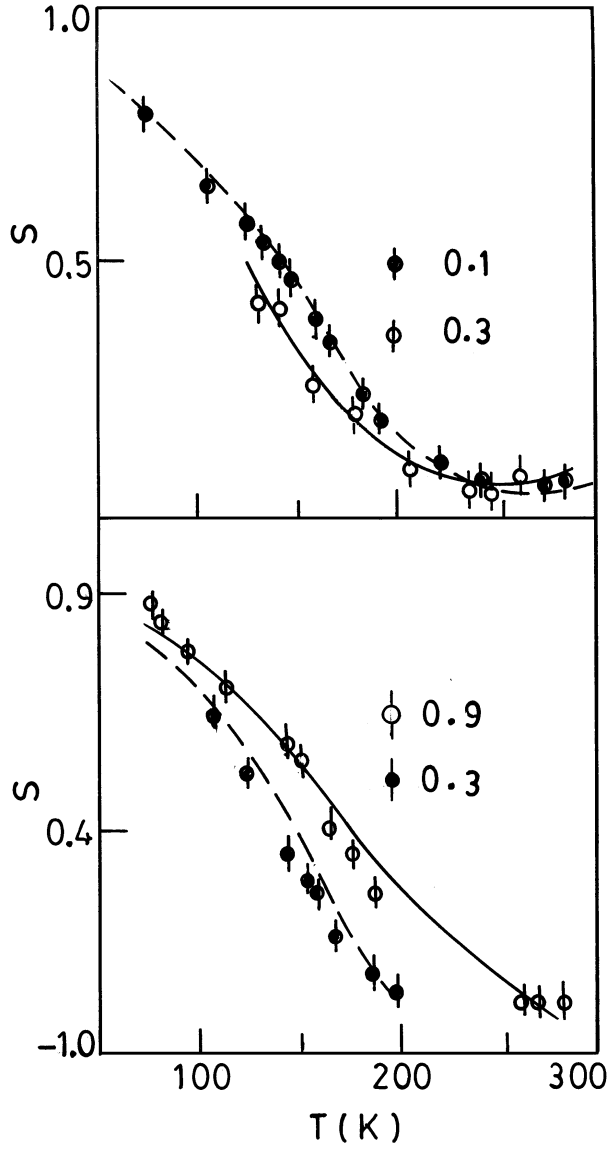

Figure 6 The thermal variation of frequency exponent (s) at 10 kHz for different compositions of the glasses fitted with OLPT model. The continuous and broken curves with error bars are the best fit curves obtained by using OLPT model (Equation 11).

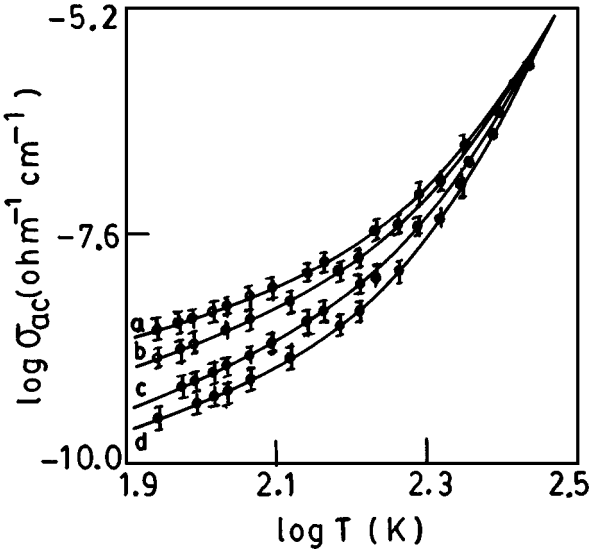

Figure 7 The log σ_{ac} vs. log T plot at 10 kHz for a typical $(1-x)$ $(90V_2O_5\text{-}10P_2O_5) + xBaTiO_3$ glass with $x = 0.1$ at different frequencies: (a) 10.0, (b) 5.0, (c) 2.0 and (d) 0.5 kHz. The continuos curves with error bars are the best fit curves obtained by using OLPT model (Equation 9).

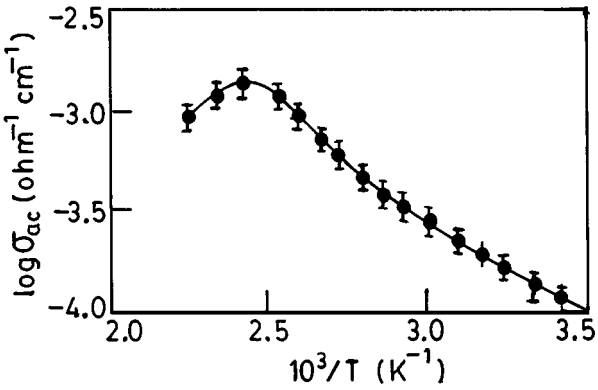

Figure 8 The thermal variation of frequency dependent AC conductivity of the $(1-x)$ $(90V_2O_5\text{-}10P_2O_5) + xBaTiO_3$ glass with $x = 0.9$ annealed at 270°C for 9 hrs (measured at 10 kHz) showing nonlinearity around 385 K which corresponds to the ferroelectric transition in $BaTiO_3$. Continuous line with error bars is a guide for the eyes.

of temperature. The thermal variation of AC conductivity of a typical $(1-x)$ $(90V_2O_5\text{-}10P_2O_5) + xBaTiO_3$ glass with $x = 0.1$ is shown in Fig. 7. To show that the nanocrystalline $BaTiO_3$ grains embedded in the glass matrix grow into larger clusters by annealing and exhibit ferroelectric type transition, we have also measured the AC conductivity of an annealed glass sample as shown in Fig. 8. A broad peak is observed around 385 K which is very close to the ferroelectric transition temperature (∼390 K) of pure $BaTiO_3$ crystal.

4. Discussion

4.1. Structural properties

X-ray diffraction patterns (Fig. 1a and b) show only broad diffuse low angle scattering which is a feature of long range structural disorder. Scanning electron microscopic study of the glasses with $x < 0.9$ also showed amorphous character. The XRD patterns of the glasses formed with $x > 0.9$, however, showed peaks of $BaTiO_3$ and TiO_2 (Fig. 1c for $x = 0.95$). The transmission electron micrograph of the glassy sample with $x > 0.9$ also indicated the presence of nanocrystalline grains (sizes varying from 40 to 60 nm) dispersed in the glass matrix. These nanocrystals are mostly $BaTiO_3$ and TiO_2 which precipitated during glass formation. Nanocrystalline phases of very low concentrations are also present in the glasses with $x < 0.9$. Very sharp crystalline rings corresponding to the nanocrystals of $BaTiO_3$ and TiO_2 (sizes varying from 50–80 nm) were also observed from the glass annealed at 300°C for 9 hrs. in air (not shown in this paper). Both crystallization (T_x) and glass transition (T_g) temperatures of the glasses dispersed with nanocrystalline phases (Table I) exhibit slow increase with increase of $BaTiO_3$ concentration. Therefore, the conductivity and strength of the glass increase slowly with $BaTiO_3$ composition which is also indicated from the little increase of density with increasing $BaTiO_3$ concentration (Table I). Appreciable shifts $(T_x - T_g)$ of T_g and T_x as shown in Table I indicate stability of these glasses. Consistent variations of density, T_g and T_x with concentration (x) also indicate the homogeneous character of the glasses.

Their spectra of the glasses are similar in nature., the corresponding ir absorption spectra of the quenched glass samples with $BaTiO_3$ are quite different from that of the pure crystalline $BaTiO_3$ as observed from Fig. 3. In the present glass system, the tetrahedron (PO_4^{3-}) exhibits two fundamental vibrational frequencies at about 1080 and 1005 cm^{-1}. The bond around 1100 cm^{-1} is considered to be a P–$O^{(-)}$ bond stretching vibration and is also called the P–O ionic stretching frequency. The bond PO_4^{3-} is present in all these glasses, whereas the bond P–$O^{(-)}$ does not appear. The bands around 785 and 490–530 cm^{-1} corresponds to P–O–P bending vibrations and harmonics of bending O–P–O and O=P–O [20].

4.2. AC conductivity

For the present VPBT glasses, the total conductivity $\sigma_t(\omega)$ measured at a particular frequency ω can be expressed as [11, 21–23]

$$\sigma_t(T, \omega) = \sigma_{ac}(T, \omega) + \sigma_{dc}(T) \qquad (1)$$

where σ_{ac}(T, ω) is the real part of the temperature and frequency dependent conductivity and $\sigma_{dc}(T)$ is the DC conductivity. Temperature dependent DC conductivity is measured independently to calculate the AC conductivity (using Equation 1). It is to be noted that Equation (1) is valid when the AC and DC contributions arise from completely separate mechanisms; otherwise the DC conductivity represents the AC conductivity in the limit $\omega \to 0$ [12]. A feature common to all amorphous semiconductors and insulators [4] is that the frequency dependent conductivity $\sigma_{ac}(\omega) \propto \omega^s$ (where the power law exponent s is generally less than or equal to unity). Many TMO glasses viz. (Bi_2O_3-CuO) [21], (V_2O_5-Bi_2O_3) [22], V_2O_5-Fe_2O_3 [23] etc. have previously been found to follow this frequency dependence even in the low frequency range.

It is evident from Fig. 4 that in the low temperature region, AC conductivity is substantially higher than the DC conductivity and it shows a weak temperature

dependence but a strong frequency dependence. On the other hand, in the high temperature region, the AC conductivity shows a strong temperature dependence but is almost frequency independent. The temperature and frequency dependence of total conductivity of the other glass compositions are also similar. It should be mentioned here that at low frequencies and high temperatures, the electrode polarization might make an appreciable contribution to the dielectric constant. However, for the present VPBT glasses, the dielectric constant is found [18] to be independent of the thickness of the samples and the electrode area for all frequencies and temperatures, indicating that the bulk effect is dominant and the electrode polarization makes no contribution to the dielectric properties. The log-log plots of AC conductivity shown in Fig. 5 are nearly straight line, indicating that the AC conductivity obeys following equation viz.

$$\sigma_{ac}(\omega) = A\omega^s, \tag{2}$$

where A is a constant dependent on temperature. This behavior demands that the loss mechanism should have a very wide range of possible relaxation times τ. From the slopes of log $\sigma_{ac}(\omega)$ vs. log ω curves (Fig. 5), the values of s are estimated and plotted in Fig. 6 as a function of temperature. The values of s for the present VPBT glasses are found to be less than unity and depends both on frequency and temperature (values of s decrease with increase of temperature which agrees with the OLPT model as discussed below).

It is well known [12] that the AC conductivity of a system is governed by the relaxation mechanism. In the transition metal ions glasses the dipole formed between two different valence states acts as relaxing species, which have a distribution of relaxation time as its length changes with the distribution of sites. It is generally assumed [12] that a Debye-type dielectric response with a distribution of relaxation times is responsible for electrical conduction. The overall conductivity is then the summation of individual microscopic processes acting in parallel. If the distribution of relaxation time τ is $n(\tau) \propto 1/\tau$, the real part of the frequency dependent conductivity obeys a linear frequency dependence. Any deviation from the linearity discloses information on the particular type of loss mechanism involved in the process. However, in models developed for different microscopic relaxation processes [11, 12], it is assumed that the relaxation is due to transfer of charge carriers in pairs (i.e. pair-approximation type model holds). Two distinct processes have been proposed [13] for the relaxation mechanism to account for the relaxation of dipoles viz., classical hopping over a barrier of charge carrier and the quantum mechanical tunneling (QMT) through barrier separating two equilibrium sites. Analysis of the $\sigma_{ac}(\omega)$ data of the semiconducting TMO glasses are generally made in the framework of QMT, correlated barrier hopping (CBH) model and overlapping large polaron tunneling (OLPT) model. In the following sections, the frequency and temperature dependent conductivity data and the exponent (s) have been analyzed in terms of these models to determine the most probable conduction mechanism in the VPBT glasses dispersed with the nanocrystalline phases.

4.3. AC conductivity and classical hopping model

The relaxation time for the classical hopping is given by $\tau = \tau_o \exp(W/k_B T)/\cosh(E_g/k_B T)$, where E_g is the energy difference between two sites [12]. Here hopping between two energetically favorable sites over a potential barrier may take place on the glasses. If the favorable sites having separation R are correlated then there is lowering of the barrier height due to Coulomb interaction [24] from W_M to $W_M - e^2/\pi\varepsilon\varepsilon_o$, where ε_o is the free-space dielectric permittivity and ε is the dielectric constant. The AC conductivity due to the CBH of an electron in the narrow band limit of this model is given by the following expression [12]

$$\sigma_{ac}(\omega) = (\pi^3/24)N^2\varepsilon\varepsilon_o\omega R_\omega^6 \tag{3}$$

where N is the concentration of localized sites. The hopping length R_ω is given by

$$R_\omega = (e^2/\pi\varepsilon\varepsilon_o)/[W_M + k_B T \ln(\omega\tau_o)] \tag{4}$$

The frequency exponent s is evaluated from the relation

$$s = 1 - 6k_B T/[W_M + k_B T \ln(\omega\tau_o)] \tag{5}$$

According to the CBH model (Equation 5) the frequency exponent s is a function of both temperature and frequency. Using W_M and τ as parameters, the experimental data are fitted with Equation (5). This model was found to fit the low temperature (below 160 K) conductivity data of the VPBT glasses. The values ($\sim 10^{-10}$ sec) of τ obtained from this model for the present VPBT glasses are also found to be one to two orders of magnitude higher ($\sim 10^{-11}$–10^{-12} sec) than those of other vanadate glasses [5, 24–26]. So we have tried to fit the experimental conductivity data other models as discussed below.

4.4. Ac conductivity and quantum mechanical tunneling model

According to QMT model [27–30] $\sigma_{ac}(\omega)$ varies linearly with temperature and the expression for the AC conductivity can be expressed as

$$\sigma_{ac}(\omega) = Ke^2 k_B T[N(E_F)]^2 \omega R_\omega^4 (1/\alpha) \tag{6}$$

where $N(E_F)$ is the density of states at the Fermi level, K is a constant factor and e is the electronic charge. The expression for frequency exponent (s) and the characteristic tunneling distance (R_ω) are given by

$$s = 1 + 4/\ln(\omega\tau_o) \quad \text{and} \quad R_\omega = (1/2\alpha)\ln(1/\omega\tau_o) \tag{7}$$

Equation 6 predicts s independent of temperature. One finds $s \sim 0.81$ for $\omega = 10^4$ rad s^{-1} and $\tau_o = 10^{-13}$ s, while s decreases as ω increases. The experimental s

value is, however, found to be temperature dependent which contradicts to the predictions of the QMT model.

It is known that in most amorphous materials a polaron is formed due to the lattice distortion [4] which was ignored in the previous approach. If small polarons are formed, the tunneling model [4] predicts a decrease in s with decrease in temperature. On the other hand, when overlapping large polarons are formed, the tunneling model [11] predicts a decrease in s with increase in temperature upto a certain range and then an increase in s with a further increase in temperature.

This was actually observed in some glassy oxide semiconductors and the AC conductivity data were analyzed by Long *et al*. [11, 27] with overlapping large polaron tunneling (OLPT) model. For such polarons, overlap of the potential wells of neighboring sites is possible because of the long range nature of the dominant coulomb interaction. Then the hopping energy will take the form [31]

$$W = W_{\mathrm{Ho}}\,(1 - r_{\mathrm{p}}/R) \tag{8}$$

where $W_{\mathrm{Ho}} = e^2/4\varepsilon_{\mathrm{p}} r_{\mathrm{p}}$, $1/\varepsilon_{\mathrm{p}} = 1/\varepsilon_{\infty} - 1/\varepsilon_{\mathrm{s}}$, ε_{s} and ε_{∞} are the static and high frequency dielectric constants respectively. r_{p} is the polaron radius and R is the mean distance between centers. The AC conductivity data of very few TMO glasses were found to be fitted with the OLPT model [27]. The expression derived by Long [11, 27] can be written as

$$\sigma_{\mathrm{ac}}(\omega) = (\pi^4/12)e^2(k_{\mathrm{B}}T)^2[N(E_{\mathrm{F}})]^2\omega R_{\omega}^4 \big/ \big[2\alpha k_{\mathrm{B}}T + (W_{\mathrm{Ho}} r_{\mathrm{p}}/R_{\omega})^2\big] \tag{9}$$

The optimum hopping length R_{ω} is calculated from the quadratic equation

$$R_{\omega}'^2 + [\beta W_{\mathrm{Ho}} + \ln(\omega\tau_{\mathrm{o}})]R_{\omega}'^2 - \beta W_{\mathrm{Ho}} r_{\mathrm{p}}' = 0 \tag{10}$$

where $R_{\omega}' = 2\alpha R_{\omega}$, $r_{\mathrm{p}}' = 2\alpha r_{\mathrm{p}}$ and $\beta = 1/k_{\mathrm{B}}T$.

The frequency exponent s is obtained from the following relation

$$s = 1 - \big[4 + 6W_{\mathrm{Ho}} r_{\mathrm{p}}'/R_{\omega}'^2\big]\big/\big[1 + \beta W_{\mathrm{Ho}} r_{\mathrm{p}}'/R_{\omega}'^2\big)^2 (1/R_{\omega}')\big] \tag{11}$$

According to this model s is both temperature and frequency dependent (Equation 11) in line with the experimentally observed values of s as shown in figure (6) for different glass samples and at a fixed frequency (10 kHz). The values of s decrease with increasing temperature and after showing a minimum value it also increases. This type of variation of s is also exhibited by the Equation 11 as shown by the theoretical fitting curve (continuous line in Fig. 6). This suggests the Long's OLPT model is an appropriate one describing the temperature dependence of s for the present VPBT glass system. The theoretical fitting parameters are shown in Table II. We also fitted the conductivity data with PLCM model. The log-log plots of experimental $\sigma_{\mathrm{ac}}(\omega)$ data and temperature (T) for a typical VPBT glass (with $x = 0.1$) are shown in Fig. 7 together with the theoretical curves (continuous lines) fitted with (Equation 9).

TABLE II Fitting parameters obtained by fitting the temperature dependent ac conductivity data of the $(1-x)(90V_2O_5\text{-}10P_2O_5) + x BaTiO_3$ glasses with the OLPT model

Value of x	α (Å^{-1})	$N(E_{\mathrm{F}})$ ($\text{eV}^{-1}\,\text{cm}^{-3}$) $\times 10^{19}$	Rω (Å)	$r_{\mathrm{p}}' = \alpha r_{\mathrm{p}}$	W_{Ho} (eV)
0.1	0.069	4.86	2.566	0.269	0.471
0.3	0.042	2.902	2.595	0.315	0.313
0.5	0.030	1.212	2.606	0.235	0.303
0.9	0.040	2.09	2.356	0.211	0.439

Maximum errors in the estimation of W_{Ho}, r_{p}', R, $N(E_{\mathrm{F}})$, and α are ±5%, ±5%, ±5%, ±2% and ±5%, respectively.

It is seen from Fig. 7 that the agreement between the theory and the experiment for the entire temperature range is very good. The corresponding fitting parameters as shown in Table II are also consistent with those obtained for similar other transition metal oxide glasses [5, 25–27]. The values of W_{Ho} decrease with increase of $BaTiO_3$ content of the VPBT glasses and are consistent with dc activation energy [18]. It should be mentioned here that OLPT model was also found to be valid for the undoped V_2O_5-P_2O_5 [26] glasses. Thus addition $BaTiO_3$ does not change the basic conduction mechanism of the vanadium phosphate glass. However, the stability of the $BaTiO_3$ containing VPBT glasses are very high compared to the pure V_2O_5-P_2O_5 glasses.

Finally, to see the effect of annealing the glass sample on the conductivity of the nanocrystal dispersed VPBT glasses, AC conductivity of some of the annealed glass-samples have also been measured between 300–400 K. By annealing the VPBT glasses at 270°C for 9 hrs. in air, the size as well as concentration of the nanocrystals increase and sharp peaks of $BaTiO_3$ and TiO_2 appear in the XRD patterns (similar to that shown in Fig. 1c). The conductivity of the annealed VPBT glass increases by about two orders of magnitude from that of the corresponding as-quenched glass. This is due to the increase of the size and concentration of the crystalline grain/clusters by annealing. It was previously reported [34] that in ceramic compound, the conductivity increases in their nanocrystalline phases. The nature of thermal variation of conductivity of a typical VPBT sample ($x = 0.9$ with maximum $BaTiO_3$ content) annealed at 270°C is shown in Fig. 8. A small and broad anomaly around $T = 390$ K is well indicated from Fig. 8. Interestingly, this anomaly corresponds to the ferroelectric transition occurring in bulk $BaTiO_3$ crystal around the same temperature [35].

5. Summary and conclusion

Ferroelectric $BaTiO_3$ doped semiconducting $(1-x)(90V_2O_5\text{-}10P_2O_5) + xBaTiO_3$ (or VPBT) glasses can be prepared for a wide range of $BaTiO_3$ concentrations ($x = 0$–0.95). These glasses are found to contain nanocrystalline $BaTiO_3$ and TiO_2 phases uniformly dispersed in the glass matrix. Unlike many conventional semiconducting TMO glasses, the frequency and temperature dependent AC conductivity data of the VPBT glasses follow the overlapping large polaron tunneling (OLPT) model. Interestingly, AC conductivity of

the partially annealed sample (at 270°C for nine hrs.) increases by a factor of about two showing a broad peak around 390 K. This broad peak around 390 K is associated with the relaxor type ferroelectric transition of the nano and micro-crystalline $BaTiO_3$ particles. It was, however, reported earlier that AC conductivity of the V_2O_5-P_2O_5 glasses does not change appreciably by annealing around 300°C [36]. This behavior is in sharp contrast to that of the present glassy system where an increase of conductivity is observed by annealing which is considered to be due to the presence of nanocrystalline phase present in the glass. Unlike the behavior of many other transition metal oxide glasses, the present glassy system shows very high (comparable to the $BaTiO_3$) dielectric constant [18] (to be discussed in our next paper). This is also considered to be due to the precipitation of nano-crystalline $BaTi0_3$ and TiO_2 phases in the VPBT glasses during glass formation. It has been reported earlier Zang *et al*. [37] that nanocrystalline $Ti0_2$ shows much larger dielectric constant than the corresponding bulk sample which is also supported by the present experimental results.

Acknowledgment

One of the authors (D. K. Modak) is grateful to the Council of Scientific and Industrial Research for financial assistance to complete the work.

References

1. J. LIVAGE, J. P. JOLIVET and E. TRONE, *J. Non. Cryst. Solids* **121** (1990) 35.
2. A. GHOSH, *J. Appl. Phys.* **64** (1988) 2652.
3. Y. SAKURI and J. YAMAKI, *J. Electrochem. Soc.* **132** (1990) 512.
4. N. F. MOTT and E. A. DAVIS in "Electronic Process in Non-Crystalline Materials" (Oxford, Clarendon Press, 1979).
5. M. SAYER and A. MANSINGH, *Phys. Rev. B* **6** (1979) 4629.
6. E. TRONE, A. MANSINGH, R. P. TANDON and J. K. VAID, *Phys. Rev. B* **21** (1980) 4829; *J. Phys.* **C9** (1976) 1809.
7. A. MANSINGH, *Bull. Mater. Sci.* **2** (1980) 325.
8. G. S. LINSLEY, A. E. OWEN and A. M HAHATEE, *J. Non. Cryst. Solids* **4** (1970) 228.
9. A. I. LAKATOS and M. ABRKOWITZ, *Phys. Rev. B* **3** (1971) 1791.
10. A. E. OWEN and J. M. ROBERTSON, *J. Non. Cryst. Solids* **4** (1970) 208.
11. A. R. LONG, *Adv. Phys.* **31** (1982) 553.
12. S. R. ELLIOTT, *ibid*. **36** (1987) 135.
13. I. THURZO, B. BARANOCK and J. DONPOVEC, *J. Non. Cryst. Solids*. **28** (1978) 177.
14. L. MURAWSKI, *Phil. Mag.* **B50** (1984) L69.
15. L. MURAWSKI, C. H. CHANG and J. D. MACKENZIE, *J. Non.Cryst. Solids* **44** (1981) 91.
16. I. G. AUSTIN and N. F. MOTT, *Adv. Phys*. **18** (1969) 41.
17. S. CHAKRABORTY, A. K. BERA, S. MOLLAH and B. K CHAUDHURI, *J. Mat. Res.* **9** (1994) 1932.
18. M. SADHUKHAN, Ph.D. Thesis, Jadavpur University, Calcutta, 1998.
19. S. MOLLAH, K. K. SOM, K. BOSE, A. K. CHAKRABORTY and B. K. CHAUDHURI, *Phys. Rev.* **B46** (1992) 11075.
20. C. DAYANAND, G. BHIKSHAMAIAH and V. JAYA TYAGARAJAN, *J. Mater. Sci.* **31** (1996) 1945.
21. S. HAZARA and A. GHOSH, *J. Phys. Cond. Matt*. **9** (1997) 3981.
22. A. GHOSH, *Phys. Rev*. **B41** (1990) 1479.
23. B. K. CHAUDHIRI, K. CHAUDHURI and K. K. SOM, *J. Phys. Chem. Solids* **50** (1989) 1137.
24. G. E. PIKE, *Phys. Rev.* **B6** (1972) 1572.
25. H. ZHENG and J. I. MAKENZIE, *ibid*. **B38** (1978) 7166.
26. L. MURAWSKI, *Phil. Mag.* **B50** (1984) L69.
27. M. POLLAK and T. H. GABALLE, *Phys. Rev.* **122** (1961) 1742.
28. M. POLLAK, *ibid*. **138** (1965) 1822.
29. H. BOTTGER and V. V. BRYKSIN, *Phys. Status Solidi (b)* **70** (1976) 415.
30. A. L. EFROS, *Phil. Mag.* **B43** (1981) 829.
31. S. MOLLAH, A. K. CHAKRABORTY, S. CHAKRABORTY, K. K. SOM and B. K. CHAUDHURI, *J. Non-Cryst. Solids* **167** (1994) 192.
32. S. CHAKRABORTY, M. SADHUKHAN, D. K. MODAK, K. K. SOM, H. S. MAITI and B. K. CHAUDHURI, *Phil. Mag.* **B71** (1995) 1125.
33. I. G. AUSTIN and N. F. MOTT, *Adv. Phys.* **18** (1969) 41.
34. N. N RITTNER and T. ABRAAHAM, *Am. Ceram. Bull*. **76** (1997) 51; "Materials" (Oxford, Clarendon Press, 1979).
35. F. JONA and G. SHIRANE, in "Ferroelectric Crystals" (Pergamon Press, Oxford, 1962).
36. A. MANSINGH, J. K. VAID and R. P. TANDON, *J. Phys. C: Solid State Phys.* **8** (1975) 1023.
37. L. D. ZANG, H. F. ZHANG, G. Z. WANG, C. M. MO and Y. ZHANG, *Phys. Stat. Splodi (a)* **157** (1996) 483.

Received 25 January
and accepted 24 October 2000